Reprinted from:
JOURNAL OF APPLIED PHYSICS VOLUME 42, NUMBER 11 OCTOBER 1971

High-Pressure Phase Transition and Demagnetization in Shock Compressed Fe-Mn Alloys*

Aristos Christou† and Norman Brown
Department of Metallurgy and Materials Science and The Laboratory for the Research on the Structure of Matter, University of Pennsylvania, Philadelphia, Pennsylvania 19104
(Received 14 December 1970)

Shock deformation of Fe-Mn alloys up to 14 wt% Mn results in a shock-induced phase transformation. It has been shown that bcc martensite with manganese in the range 4–16 wt% transforms to a stable close-packed phase under pressure without the occurrence of reversion. The addition of manganese to iron also decreases the transition pressure from 133 kbar for pure Fe to less than 70 kbar for Fe–14Mn. X-ray diffraction, electron-probe microanalysis, electron microscopy, and density results indicate that for the Fe-4Mn and Fe-7Mn alloys, the fcc phase has been stabilized after shock deformation, while the ϵ phase has been stabilized for the Fe-14Mn alloy. Saturation magnetization studies have detected a residual reduction in magnetization due to the retainment of the high-pressure phase.

I. INTRODUCTION

A magnetic phase transition in iron in the vicinity of 130 kbar has been confirmed in both dynamic and static experiments.[1–3] Recent experiments indicate that a partial phase transition to the nonmagnetic ϵ phase (hcp) can occur at shock pressures as low as 50 kbar.[4] However, since iron reverts to its initial structure on relief, residual phase changes have not been observed.

The temperature-pressure diagram for iron, shown in Fig. 1, can be modified by the addition of alloying elements to iron. Specifically, the stability of the close-packed phase of iron can be increased by the addition of manganese.[5] The phase diagram is shown in Fig. 2. Magnetic susceptibility measurements[6] of Fe-Mn alloys that had been shocked at pressures up to 300 kbar indicated that the high-pressure phase could be retained at zero pressure. Since the duration of a shock-wave pressure pulse is about 10^{-6} sec, any phase transformation which occurred must be martensitic.

The present work is an investigation of the residual magnetic and crystallographic phase changes in shock-deformed iron-manganese alloys. Our experimental results are related to shock-induced martensitic and magnetic transformations. We will show that in Fe-Mn density, x-ray microstructural, and magnetization changes are due to the partial retention of the high-pressure phase.

II. EXPERIMENTAL DETAILS

A. Sample Preparation

The composition of the alloys included in this study is given in Table I. All alloys were prepared using an electrolytic grade of iron and high-purity manganese (99.9%); 0.007 wt% carbon was the main im-

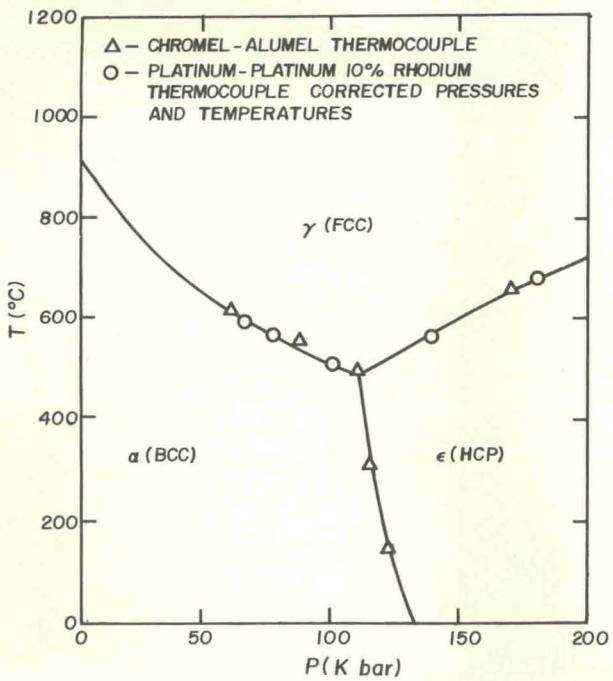

FIG. 1. Temperature-pressure diagram for iron (see Ref. 2).

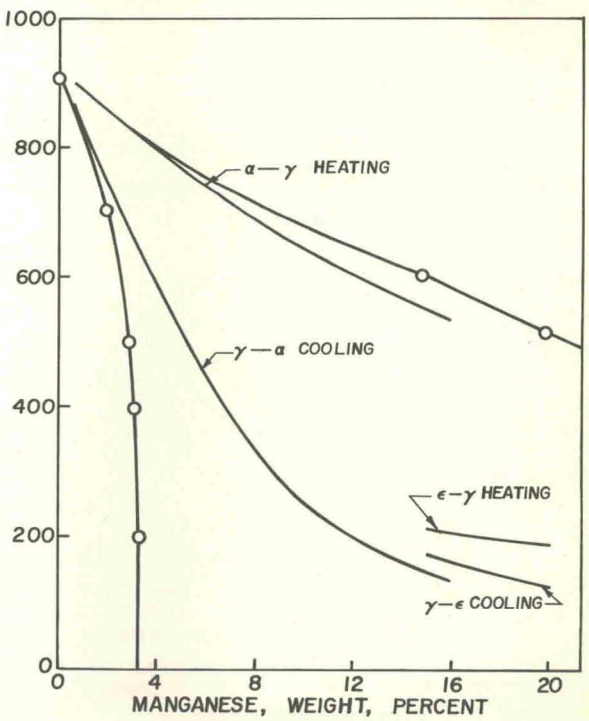

FIG. 2. Transformation and equilibrium diagram for the Fe-Mn system.

TABLE I. Composition of alloys.

Alloy designation	Composition (wt% Mn)
Fe	0
Fe-0.4Mn	0.38
Fe-4Mn	4.10
Fe-7Mn	7.37
Fe-14Mn	13.62

purity. The alloys were arc melted in an argon atmosphere under conditions which insured good homogeneity. Hot-rolled samples having dimensions 20×6.0×1.3 mm were machined and annealed for 9 h at temperatures between 900–950 °C. Half of the specimens were quenched from the austenitic region and the rest were furnace cooled to room temperature in 72 h. Plane-wave shock-deformation tests were performed at peak pressures of 90, 150, 300, and 500 kbar. The basic method of plane-wave generation has been described previously.[7]

B. Experimental Methods

Magnetization curves for shock deformed and annealed specimens were determined by standard "ring techniques" described by Rose, Villere, and Berger.[8] All measurements were taken at room temperature. The maximum applied field was 1000 Oe.

Density was measured at the National Bureau of Standards and at the Naval Weapons Laboratory using a displacement technique. Density changes of ±0.0001 g/cm^3 were detectable. The liquid used in determining the density was Di(2-ethyl hexyl) azelate.

Crystal structures and microstructures were observed with x-rays, electron probe, light, and transmission electron microscopy.

The electron probe was used to study variations of manganese concentrations and to facilitate the interpretation of the optical micrographs. The Norelco instrument was operated at 30 kV with a specimen current between 0.035 and 0.05 μA. To determine the manganese content within the bcc and close-packed phases, a calibration curve of relative intensity $(I/I_0)_{Mn}$ vs manganese content was determined using four homogeneous Fe-Mn alloys (Fig. 3). It was of interest to show that the calibration curves agree with the calculated curves of Castaing[9] and Wittry[10] who made corrections for absorption and fluorescence.

Identification of the retained high-pressure was accomplished by x-ray diffraction of powdered Fe-Mn using Mo$K\alpha$ radiation. Thin foils, suitable for examination by electron transmission microscopy, were electropolished in a solution consisting of 430 ml of H_3PO_4, 50 g of CrO_3, and 7 ml of distilled water at 0 °C and a current density of 1.2 A cm^{-2}.

III. EXPERIMENTAL RESULTS

A. Density Experiments

Density measurements are shown in Table II. Density measurements of the quenched and shock-loaded

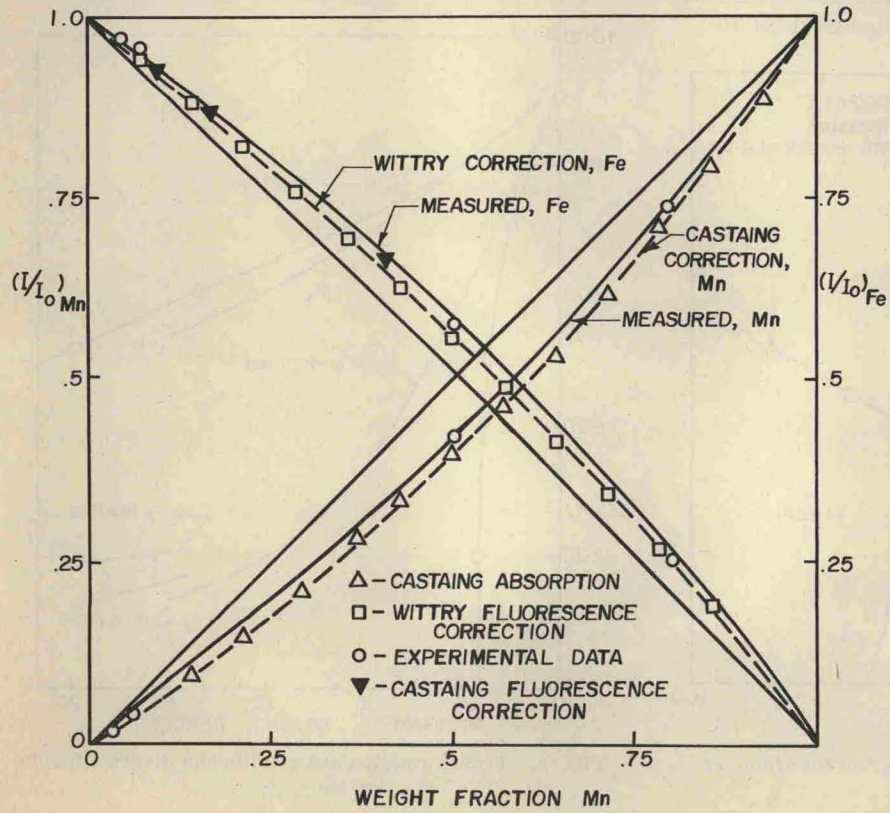

FIG. 3. Measured I/I_0 vs composition curves for the Fe-Mn system.

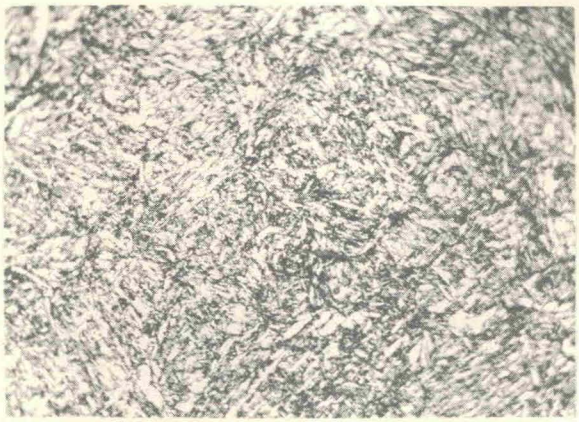

(a)

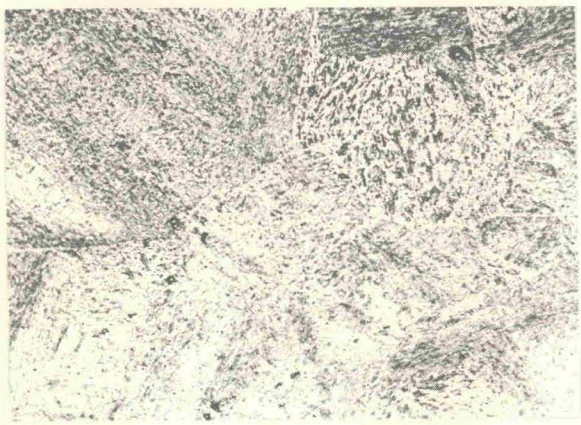

(b)

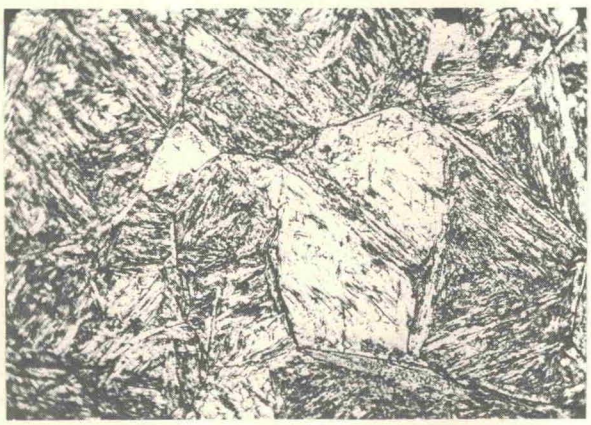

(c)

FIG. 4. (a) Typical Fe-Mn unshocked microstructure following a water quench. Magnification is 500×. Austenitic grain boundaries are hidden. (b) Shock-loaded Fe-7Mn at 300 kbar, showing mixed microstructure. Austenitic grain boundaries have reappared due to the retainment of the high-pressure fcc phase. Magnification is 500×. (c) Microstructure of the shocked Fe-7Mn. Typical martensitic structure is shown, with prior austenitic grain boundaries. Magnification is 500×.

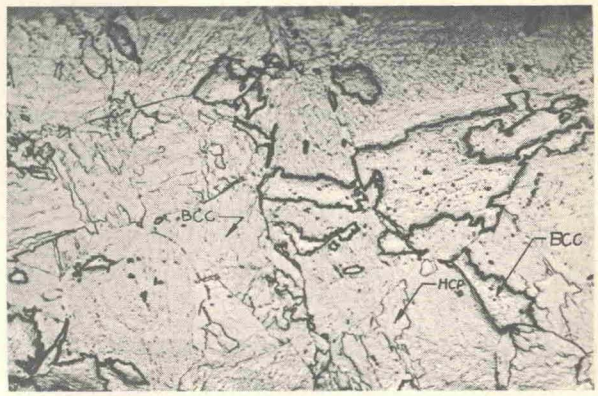

(a)

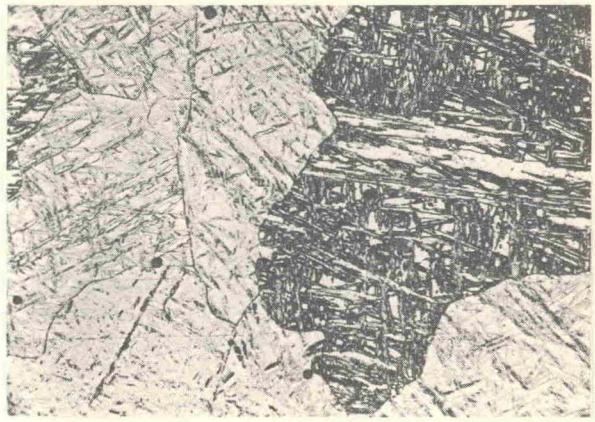

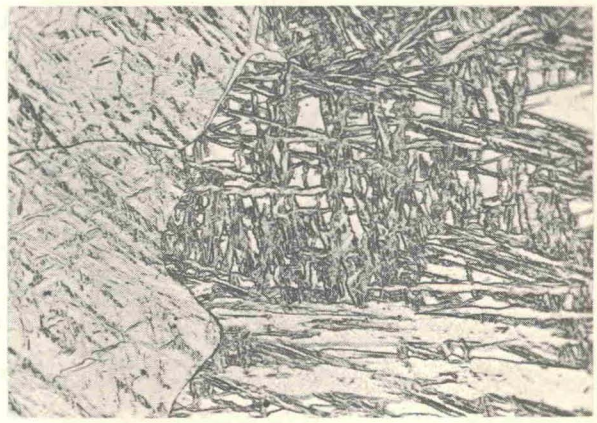

(b)

FIG. 5. (a) Microstructure of Fe-7Mn slow cooled from 900 °C. The hcp phase is outlined by the lightly etched grain boundaries. The matrix is bcc. These observations have been verified by the electron probe. Magnification is 250×. (b) Microstructure of Fe-7Mn, slow cooled and shock loaded to 300 kbar. Profuse twinning is evident. Magnification is 500×.

specimens clearly indicate that the high-pressure phase has been retained in the alloys Fe-4Mn to Fe-14Mn, which were shock loaded at pressures above 90 kbar. The maximum density change occurred after shock deformation at 300 kbar for Fe, Fe-0.4Mn, and Fe-4Mn and at 500 kbar for Fe-7Mn and Fe-14Mn. From 300–500 kbar there was no appreciable change in the retention of the close-packed phases. No appreciable density changes were observed in the Fe and Fe-0.4Mn alloys. The density change was much less in the alloys which were initially furnace cooled prior to shock deformation. The residual density changes are believed to be due to an $\alpha' \rightarrow \gamma$ or $\alpha' \rightarrow \epsilon$ transformation. The stability of the shock-

TABLE II. Density changes in shock deformed Fe-Mn alloys.

Alloy	Heat treatment	Initial density ρ_0 (g/cm^3) at 20 °C	Density changes[a] 90 kbar	150 kbar	300 kbar	500 kbar
Fe	900 °C, water quench	7.8711	1.0001	1.0002	1.0002	1.0002
Fe-0.4Mn	900 °C, water quench	7.8716	1.0002	1.0002	1.0003	1.0003
Fe-4Mn	950 °C, water quench	7.8698	1.0023	1.0097	1.0146	1.0140
Fe-7Mn	950 °C, water quench	7.9088	1.0028	1.0028	1.0218	1.0431
Fe-14Mn	950 °C, water quench	7.9902	1.0275	1.0392	1.0449	1.0450
Fe	900 °C, furnace cool	7.8712	1.0001	1.0002	1.0002	1.0002
Fe-0.4Mn	900 °C, furnace cool	7.8719	1.0002	1.0002	1.0002	1.0003
Fe-4Mn	950 °C, furnace cool	7.8722	1.0002	1.0006	1.0007	1.0007
Fe-7Mn	950 °C, furnace cool	7.9135	1.0003	1.0006	1.0007	1.0008
Fe-14Mn	950 °C, furnace cool	7.9939	1.0008	1.0008	1.0009	1.0009

[a]Density change = density after shock loading (ρ_s)/unshocked density (ρ_0).

produced close-packed phases was exhibited by quenching them to 78 °K and causing only a slight change in the density ratio (less than 0.15%). It is emphasized that the retained close-packed phase which was produced by shock primarily came from the bcc martensite with manganese content in the range of 4-16 wt%. The retained high-pressure phase increased with the manganese content of the bcc phase. The slow-cooled alloys contained bcc martensite with 2—4 wt% Mn, and, consequently, the retainment of the high-pressure phase was not possible.

B. Structure Determination

X-ray diffraction data of all alloys were taken before and after shocking at 90, 150, and 300 kbar. The x-ray diffraction results indicate that, for the Fe-4Mn and Fe-7Mn alloys, the γ phase has been stabilized at room temperature after shock deformation, while the ϵ phase has been stabilized for the Fe-14Mn alloy. The unshocked quenched Fe, Fe-0.4Mn, and Fe-4Mn specimens produced the diffraction lines of bcc Fe-Mn; equilibrium bcc and martensitic bcc lines were not separable. The α' lattice parameter was found to increase linearly with increasing solute content up to 14 wt% Mn. The unshocked quenched Fe-7Mn and Fe-14Mn specimens produced the diffraction lines of bcc martensite. The quenched and shocked Fe and Fe-0.4Mn specimens showed the same lines as the unshocked specimens. However,

TABLE III. X-ray diffraction data of Fe-Mn shock loaded up to 300 kbar.

P (kbar)	d(bcc) (Å)	$(hkl)_{bcc}$	a(bcc) (Å)	d(hcp) (Å)	$(hkl)_{hcp}$	a(hcp) (Å)	c(hcp) (Å)	d(fcc) (Å)	$(hkl)_{fcc}$	a(fcc) (Å)
Fe-14Mn										
unshocked	2.05±0.05	(110)	2.85							
	1.40±0.05	(200)								
	1.20±0.03	(211)								
150	~2.04±0.05	(110)	2.83	1.90±0.05	(101)	2.45	3.95			
	1.40±0.08	(200)		~2.00±0.06	(002)					
	~1.19±0.05	(211)								
300	~2.04±0.05	(110)	2.83	2.14±0.06	(100)	2.45	3.95			
	1.40±0.05	(200)		~2.00±0.08	(002)					
	1.17±0.07	(211)		~1.90±0.08	(101)					
				1.45±0.05	(102)					
				1.25±0.07	(110)					
				1.15±0.07	(103)					
Fe-7Mn										
unshocked	~2.00±0.02	(110)	2.80							
	1.38±0.02	(200)								
	1.21±0.03	(211)								
300	~2.00±0.05	(110)	2.80					2.06±0.05	(111)	~3.50
[Fe-7Mn]	1.40±0.06	(200)						1.80±0.05	(200)	~3.50
	1.20±0.05	(211)						1.30±0.05	(220)	~3.47
Fe-4Mn										
unshocked	~1.98±0.05	(110)	2.79							
	1.38±0.02	(200)								
	1.20±0.03	(211)								
300								2.05±0.05	(111)	~3.50
								1.79±0.05	(200)	~3.49
								1.32±0.05	(220)	~3.48

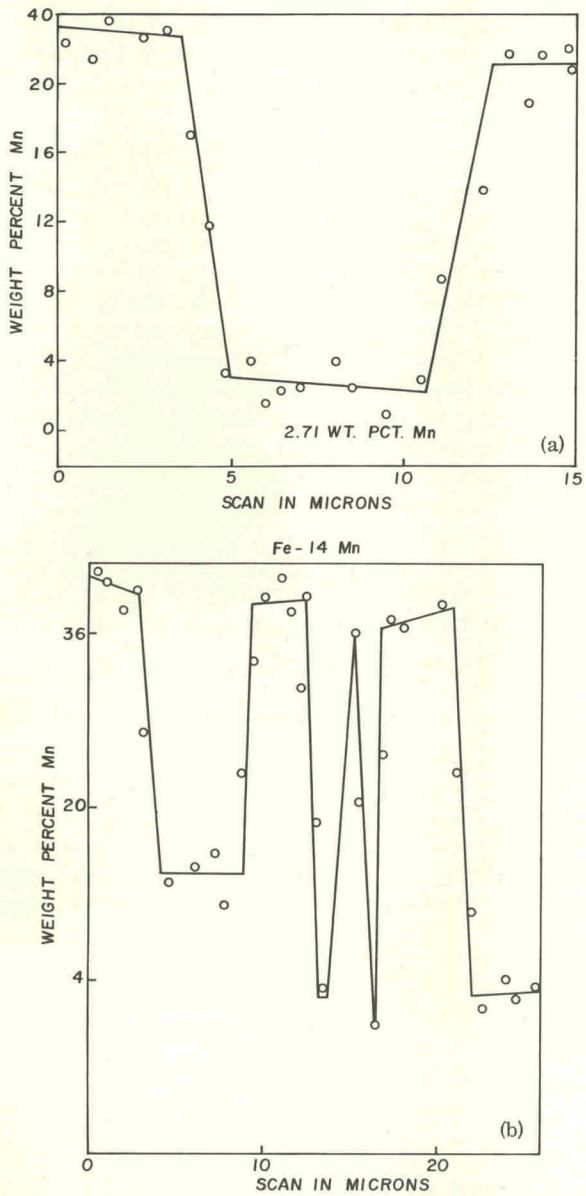

FIG. 6. Electron microprobe data on (a) Fe-7Mn and (b) Fe-14Mn specimens slow cooled and shock loaded at 300 kbar.

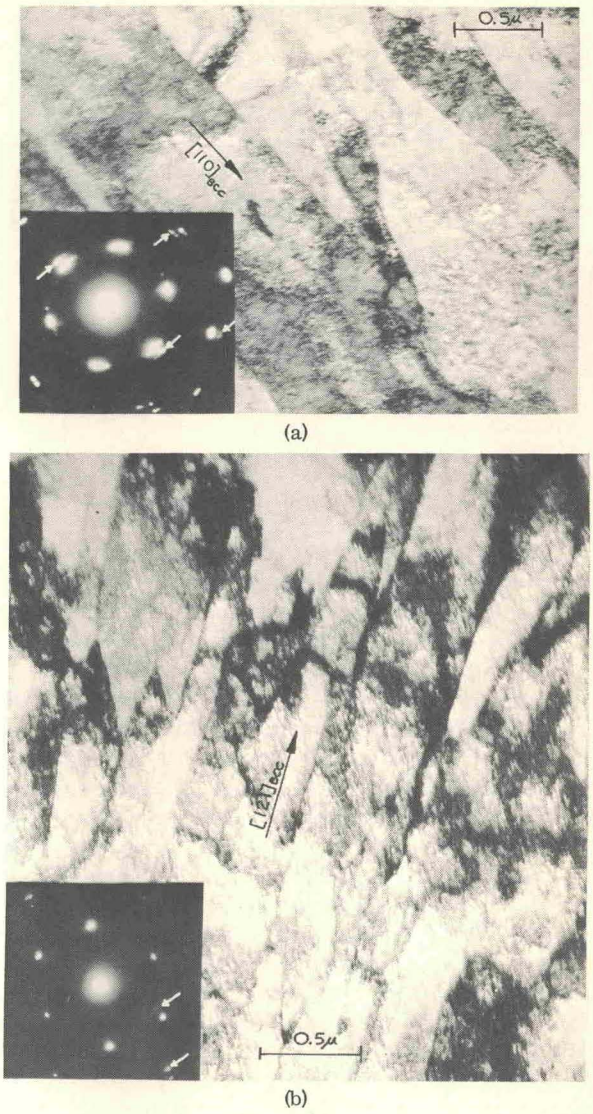

FIG. 7. (a) Electron micrograph of quenched shock-loaded Fe-7Mn at 90 kbar. The fcc plates have transformed from the initial bcc structure. The fcc plates have been identified by electron diffraction. (b) Electron micrograph of slow-cooled shock-loaded Fe-7Mn at 90 kbar.

the quenched and shocked Fe-4Mn and Fe-7Mn alloys showed bcc and fcc lines, with the lattice parameters shown in Table III. The quenched and shocked Fe-14Mn alloys showed bcc and hcp phases with the lattice parameters also indicated in Table III. Six of the lines were clearly identified as hcp with a c/a ratio of 1.61. The hcp lines identified in the Fe-14Mn alloy after the 150-kbar shock had the same c/a ratio as after the 300-kbar shock. The unshocked slow-cooled Fe, Fe-0.4Mn, and Fe-4Mn specimens produced diffraction lines of bcc martensite. The unshocked slow-cooled Fe-7Mn and Fe-14Mn alloys produced hcp martensite and bcc martensite. All alloys had a 5–10% volume fraction of untransformed fcc phase. Apparently, the hcp phase in the annealed alloys is a discrete phase, very similar to the hcp phase in cobalt. The shock loading of the slow-cooled specimens did not produce any new lines. In addition, shock loading did not change the volume fraction of each phase present in the slow-cooled alloys.

C. Microstructure

By light microscopy, the microstructure of all alloys was observed before and after shock loading to 300 kbar. Representative optical micrographs of the Fe-7Mn alloy are shown in Fig. 4. The typical martensitic structure prior to shock loading is shown in Fig. 4(a). The prior austenitic grain boundaries are not obvious, but with closer scrutiny of the changes in orientation of the martensitic plates, the austenitic grain boundaries become evident. After shocking, the prior austenitic grain boundaries are easily

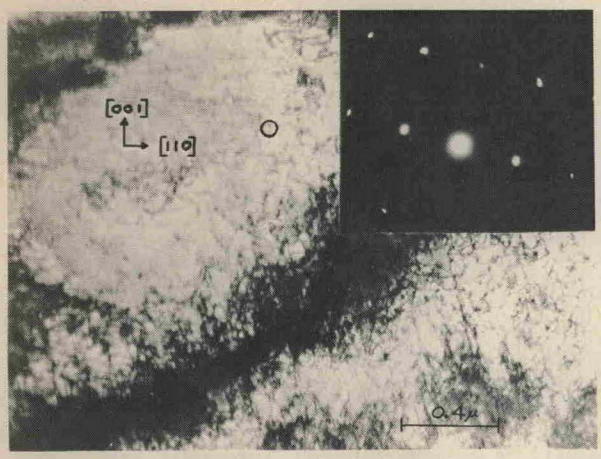

FIG. 8. Electron micrograph of shock-loaded Fe-7Mn at 300 kbar. Extensive transformation has occurred.

recognizable for the Fe-7Mn alloy [Figs. 4(b) and 4(c)]. This last observation is very important because it indicates that during shocking α' reverted to γ by the same mode of shear that occurred during quenching. In contrast to the case of Fe-7Mn, the austenitic grain boundaries in Fe-14Mn which existed prior to quenching are not visible after shocking because they are obscured by the α' to ϵ transformation. Consequently, the shocked Fe-14Mn is very nondescript. Figure 5(a) shows the structure of the slow-cooled Fe-7Mn alloy. This microstructure is typical for all slow-cooled alloys. The lightly outlined grains represent the hcp phase, while the matrix is the bcc phase. These phases have been identified by the electron probe and will be discussed in Sec. IV. Figure 5(b) shows the slow-cooled structure for Fe-7Mn after shock loading at 300 kbar. This microstructure is typical for all shocked furnace-cooled alloys. The prominent feature of the shocked furnace-cooled alloys is the presence of profuse twinning, and there is no retained high-pressure phase in the furnace-cooled specimens as supported by the density and x-ray observations.

The electron-probe microanalysis, while facilitating the interpretation of the optical micrographs, also indicated the distribution of manganese in the shocked and unshocked specimens. The manganese variation was measured in shocked specimens, and those which were only quenched or furnace cooled. Segregated regions were observed in both the 7 and 14 wt% Mn alloys furnace cooled from 900 °C. The type of segregation was the same in both the shocked and unshocked furnace-cooled specimens. The segregated regions in the furnace-cooled shock-loaded Fe-7Mn alloy were 5–15 μ long with manganese concentration changing discontinuously from 2.5 to 23.0 wt% [Fig. 6(a)]. Similarly segregated regions in the Fe-14Mn furnace-cooled shock-loaded specimens were also 5–15 μ long with a variation in manganese concentration from 3.5 to 40 wt% [Fig. 6(b)]. These variations are consistent with the manganese content in α and γ as predicted by the phase diagram. The manganese distribution in the quenched alloys was homogeneous and segregated regions were not detected. The quenched and then shocked alloys had the similar homogeneous distribution of manganese.

The microstructure of Fe-4Mn, Fe-7Mn, and Fe-14Mn was studied using the electron microscope. One alloy (Fe-7Mn) will be described in detail because its microstructure is representative of all alloys. The Fe-7Mn specimens which were shock loaded at 90 and 300 kbar showed fcc and bcc phases [Figs. 7(a) and 7(b)]. The fcc phase was identified by selected-area diffraction methods. The fcc phase was in the form of platelike islands of retained austenite within the martensite matrix. These plates of austenite were formed by shocking because no austenite existed in the as-quenched state. At 300 kbar, the amount of fcc was much greater as shown in Figure 7(b), as expected from the density measurements. On the other hand, the furnace-cooled Fe-7Mn specimens shocked to 90 kbar did not show retained fcc, as shown in Fig. 8, and were characterized primarily by a cellular dislocation structure. Shock loading the furnace-cooled specimens at 500 kbar resulted in the formation of subgrains indicating that some recovery had taken place during the shock loading.

The diffraction pattern of Fig. 7(a) (Fe-7Mn, 90 kbar) is primarily bcc resulting from the matrix. The fcc spots are marked on the pattern and indicate that the retained fcc cells are elongated in the same

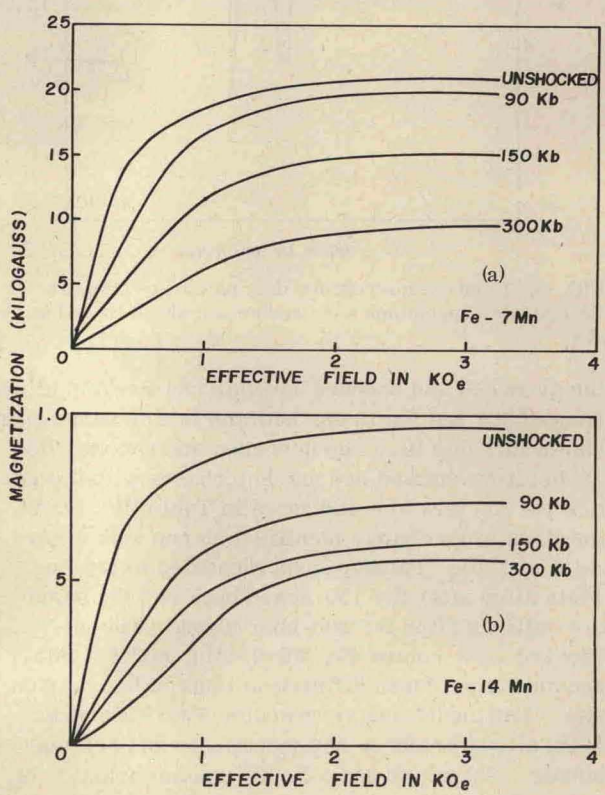

FIG. 9. Magnetization curves for shock-deformed Fe-Mn alloys: (a) Fe-7Mn and (b) Fe-14Mn.

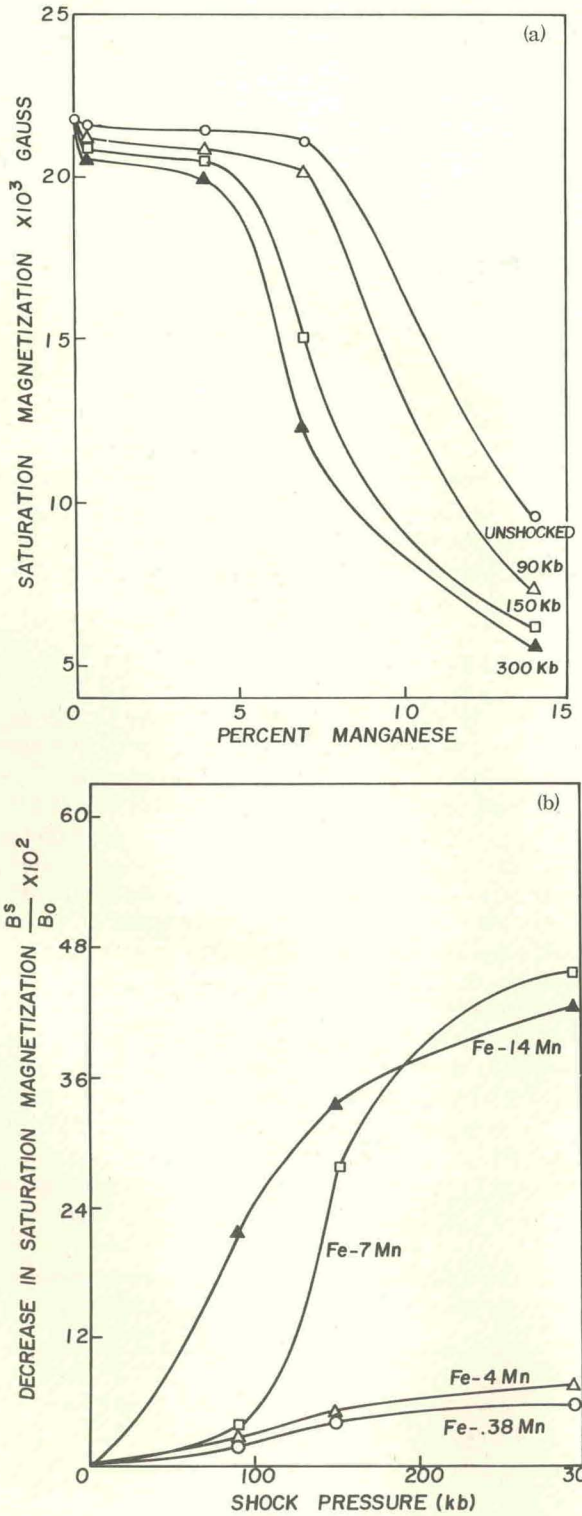

FIG. 10. (a) Saturation magnetization as a function of manganese content for shocked and unshocked alloys. (b) Fractional change in saturation magnetization as a function of peak pressure.

direction and are aligned along the $[110]_{bcc}$. The diffraction pattern of Fig. 7(b) (Fe-7Mn, 300 kbar) is primarily fcc; and, when the bcc and fcc diffraction patterns are superimposed, the following crystallographic relationship was obtained:

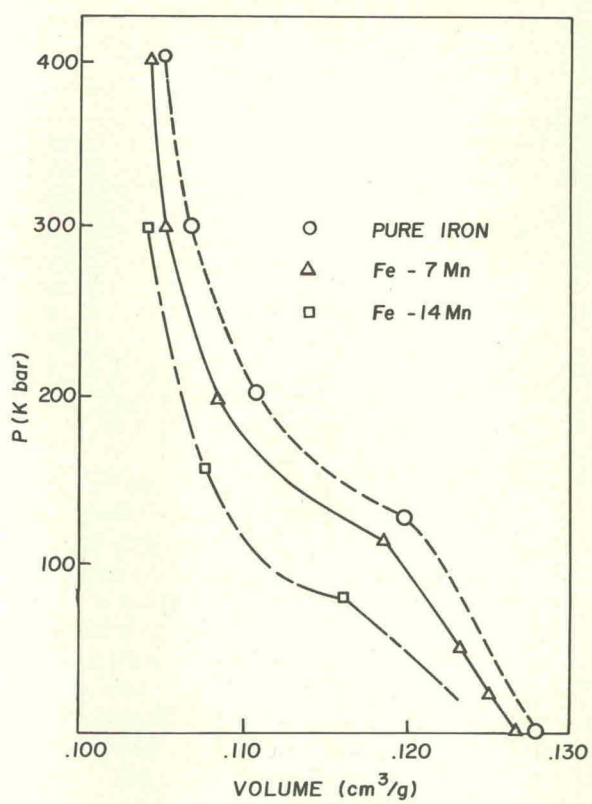

FIG. 11. Hugoniot curves for Fe-Mn alloys.

$$[\bar{1}11]_\gamma \| [110]_m, \quad (101)_\gamma \| (\bar{1}1\bar{1})_m. \tag{1}$$

This orientation relationship corresponds to that of Kurdjumov and Sachs.

The habit plane of the fcc phase in shocked Fe-7Mn was determined by single surface trace analysis. Two different types of habit planes were observed at 90 kbar. Five habits were approximately $(\bar{1}\bar{1}2)_\gamma$ and only one was near $(\bar{2}\bar{2}5)_\gamma$. At 150 kbar, for the variant of the orientation relationship used, the habit plane was always found to be near $(\bar{1}\bar{1}2)_\gamma$.

D. Magnetization Measurements

The magnetization curves appearing in Fig. 9 indicate different approaches to saturation at each pressure. In general there is a lowering of saturation magnetization with increasing shock pressure, as shown in Fig. 10(a). The fractional decrease in saturation magnetization is shown in Fig. 10(b). The greatest fractional change in saturation magnetization occurred for the Fe-7Mn alloy, which was shocked at 300 kbar. However, at 150 kbar the change in saturation magnetization was greater for the Fe-14Mn than for the Fe-7Mn alloy. This observation is consistent with the density measurements. Figure 10(a) shows that the saturation magnetization changes only slightly with shock pressure when the manganese content is below 4 wt%. This means that the change in the B-H curve produced by dislocations is relatively small compared to the change produced

TABLE IV. Retained high-pressure phases of the quenched alloys.

Alloy	Pressure (kbar)	Vol% fcc		Vol% hcp	
		Density	Magnetization	Density	Magnetization
Fe-4Mn	90	2.25	3.10		
	150	10.80	6.50		
	300	16.25	11.00		
	500	15.50	13.50		
Fe-7Mn	90	3.12	3.20		
	150	25.25	24.00		
	300	47.50	45.00		
	500	47.60	47.00		
Fe-14Mn	90			30.10	25.00
	150			38.00	34.50
	300			49.20	44.00
	500			49.20	45.00

by the retention of the close-packed paramagnetic phases. For the Fe-7Mn alloy, as shown in Fig. 10(a), and decrease in saturation magnetization between 90 and 150 kbar is the result of the $\alpha' \rightarrow \gamma$ transformation. In the Fe-14Mn alloy, a significant decrease in saturation magnetization occurs below 90 kbar. It is likely that the transformation was initiated below 90 kbar for the Fe-14Mn alloy. The decrease is saturation magnetization with shock pressure for the Fe-14Mn alloy is caused by the retention of the close-packed phase.

IV. DISCUSSION

A. Discussion of Experimental Results

The density data, magnetic data, and microstructure all show that close-packed phases can be retained after shock loading if the unshocked specimens contained bcc martensite, with the manganese content in the range 4–16 wt%. Alloys which were slow cooled did not retain the high-pressure phase after shock loading because their bcc martensite contained less than 4 wt% Mn. In addition, the slow-cooled alloys already contained a close-packed phase prior to shock loading. Therefore, manganese in bcc martensite, between 4 and 16 wt% stabilizes the high-pressure close-packed phases. It is of interest to calculate the amount of retained phases based on the different types of measurements.

From the rigid-sphere model, a theoretical density change for $\alpha \rightarrow \gamma$ is 8.98% and for $\alpha \rightarrow \epsilon$ is 9.12%. Using the density measurements of Table II, the percentages of retained high-pressure phases have been calculated as shown in Table IV. The amount of retained high-pressure phases can also be estimated from the magnetization measurements, based on the difference in saturation magnetization between the shocked and unshocked specimens (Table IV). It is to be noted that the estimate of the amount of retained high-pressure phase from the density and magnetic data is the same. Table II shows that all alloys, and even the pure iron, showed an increase in density after shock loading. It would appear that the density changes from 1.0001 to 1.0003 may be a result of microvoid coalescence.[11,12] Possibly the density changes which were observed in the furnace-cooled alloys with 4–14 wt% Mn may be caused by very small amounts of retained high-pressure phases which were not detectable by the other methods of

TABLE V. Retained high-pressure phases in alloys.

Alloy	Heat treatment	Phase transformation	Habit plane and shear system
Fe-32 Wt% Ni (Ref. 20)	LNQ[a]	$\alpha' \rightarrow \gamma$	$\sim(5\bar{2}3)\alpha$ $(110)\gamma\ [1\bar{1}0]\gamma$
Fe-Ni-C (Ref. 20)	LNQ	$\alpha' \rightarrow \gamma$	$(225)\gamma$ $(110)\gamma\ [1\bar{1}0]\gamma$
			$(11\bar{2})\gamma$ $(111)\gamma\ [\bar{1}2\bar{1}]\gamma$
Fe-7Mn, Fe-4Mn (present work, Ref. 6)	Water quench	$\alpha' \rightarrow \gamma$	$(\bar{1}\bar{1}2)\gamma$(Fe-7Mn) $(111)\gamma\ [\bar{1}2\bar{1}]\gamma$
Fe-14Mn		$\alpha' \rightarrow \epsilon$	...
Ti-Mo (Ref. 22)	LNQ	$\alpha \rightarrow \epsilon$	...
Ti-V (Ref. 22)	LNQ	$\alpha \rightarrow \epsilon$	...

[a]Liquid-nitrogen quench.

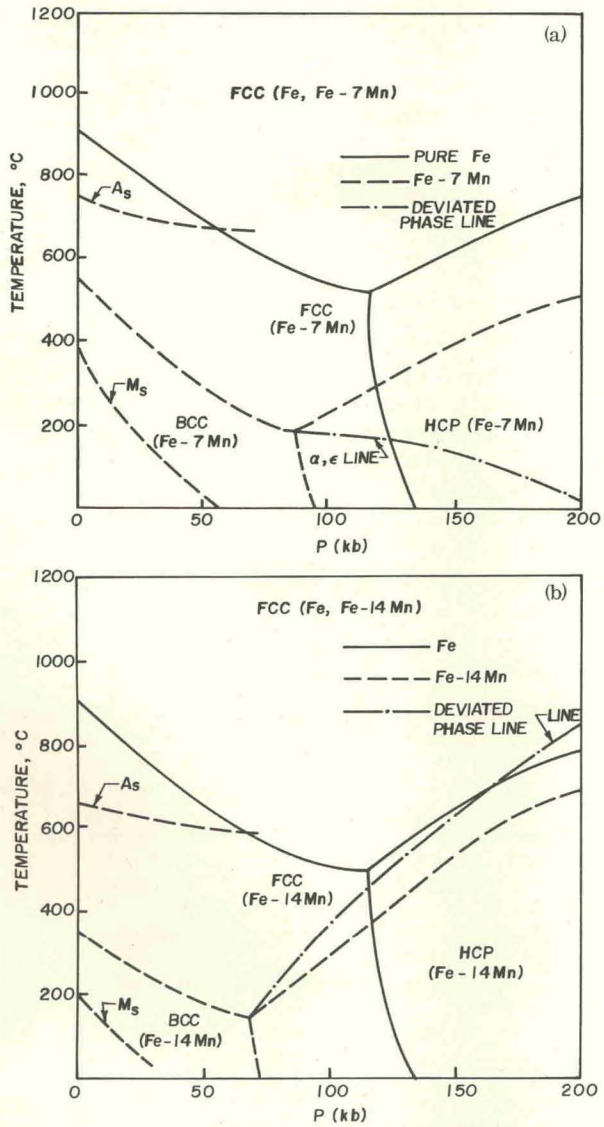

FIG. 12. Equilibrium temperature-pressure diagram for Fe-Mn showing the effect of manganese on the triple point: (a) Fe-7Mn and (b) Fe-14Mn.

observation. It is of interest to calculate the change in density which is produced only by shock-generated dislocations and point defects. The density change from dislocations[13] is given by

$$\Delta D/D = \tfrac{3}{2} b^2 \rho_D, \tag{2}$$

where ρ_D is the density of dislocations, D is the material density, and b is the Burgers vector. Using the dislocation density observed for iron at 300 kbar, a decrease in $\Delta D/D$ of 7.3×10^{-5} should result. This value is too small to be observed experimentally, and by itself it should have produced a decrease in density, while an increase was observed in the present case. The point-defect density based on the observations of Kressel and Brown[14] is too small to be observed experimentally.

Saturation magnetization of annealed Fe-Mn alloys as measured previously[15] is consistent with the results of this investigation and showed a sudden change in the slope of the saturation magnetization vs manganese curve at 7 wt% Mn. Shock deformation produces a significant drop in the saturation moment when the wt% Mn concentration exceeds 4%, as shown in Fig. 10(b). This drop occurs at all shock pressures. It should be noted that after shock deformation, the approach to saturation is more gradual due to the dislocations and point defects produced by the shock. This factor increases the uncertainty in the location of the saturation field, and it is probable that saturation was not actually reached at fields of 1000 Oe. Thus the decrease in saturation magnetization after shock loading Fe-0.4Mn should be attributed to dislocations and point defects rather than to a retained close-packed phase.

Density, saturation magnetization, and susceptibility[6] measurements indicate that the transformation occurs at pressures below 90 kbar. This agrees with the work of Keeler and Mitchell[4] who found that a partial phase transition to the nonmagnetic hcp phase can occur at shock pressures as low as 50 kbar. It is obvious that the addition of manganese to iron lowers the transition pressure. This is consistent with the magnetization data of Fig. 10(b). It is noted in Fig. 10(b) that the changes in saturation magnetization for the Fe-14Mn alloy occurs well below 90 kbar, and for the lower manganese alloys the transformation seems to occur at about 90 kbar. The transformation pressures, according to the Hugoniot curves of Fig. 11,[16,17] are generally higher for each corresponding manganese content.

Bowden and Kelly[18] using electron microscopy have studied the pressure-induced phase transformation in Fe-C and Fe-Ni-C. In the case of Fe-Ni-C it was found that the high-pressure phase was fcc, which was retained after the passage of the shock wave. These authors, however, were not able to retain the high-pressure phase in the Fe-C alloys. In a separate study Leslie, Stevens, and Cohen[19] were able to retain the high-pressure fcc phase of a shock-loaded α-martensite Fe-32% Ni alloy. Bowden and Kelly[18] found that under shock-loading conditions, α' transforms to γ by an exact reversal of the original transformation which produced the α' martensite. This finding is consistent with our optical observations on the Fe-7Mn alloy. Koul and Breedis[20] likewise were able to retain high-pressure phases of shocked titanium alloys. It is also noted that a commercial method of producing diamonds is based on the retention of the high-pressure phase after shock loading. Table V summarizes previous work done on retained high-pressure phases in alloys.

B. Thermodynamic and Stability Considerations

The results of the present investigation have shown that the high-pressure phase has been retained after the passage of the shock wave. The addition of manganese to iron has modified the temperature-pres-

sure diagram by increasing the field of stability of the fcc and hcp phase. Therefore, the shock loading of a bcc-martensite structure with an appropriate solute content results in an $\alpha' \rightarrow \gamma$ or $\alpha' \rightarrow \epsilon$ transformation. Figure 12 shows that the triple point has been lowered to about 90 kbar for Fe-7Mn and 70 kbar for Fe-14Mn, and hence the fcc and hcp fields have been greatly stabilized with respect to the bcc phase. The T_0-P lines for the Fe-7Mn and Fe-14Mn alloys as a first approximation were drawn parallel to the phase lines for pure iron, and were also made to pass through the two experimentally known states $(T_0, P=0)$ and (T_c, P_c). The presure P_c is the transformation pressure obtained from the Fe-Mn Hugoniot, and T_c is the temperature of the compressed solid at P_c calculated using the equations of McQueen *et al.*[21] From the present observations the phase line between the fcc and hcp phase must deviate as shown in Fig. 12 so as to explain the room-temperature stability of fcc for Fe-7Mn and hcp for Fe-14Mn.

The calculation of the initial P-T_0 slope ($P=0$, $T=T_0$) for Fe-7Mn and Fe-14Mn is based on the Calusius-Clapyron equation. The initial PT slope for the bcc$\rightarrow$ fcc transformation has the following values:

$$\left(\frac{dT}{dP}\right)^{\alpha\rightarrow\gamma} = -10.5\ ^\circ\text{K/kbar}.$$

The enthalpy change $\Delta H_{\alpha\rightarrow\gamma}$ and the entropy change $\Delta S_{\alpha\rightarrow\gamma}$ are functions of temperature and solute concentration.[22] Therefore the slope of the P-T_0 curve will deviate from the initial dT/dP slope and from the slope of the pure-iron phase lines.

In addition to the thermodynamic considerations, dislocations generated by (a) the quench and (b) shock deformation and their interactions may stabilize the high-pressure phases. The first set of dislocations produced during quenching will have an internal stress field which is related to the shear mechanism during the martensitic transformation via quenching; an entirely different set of dislocations is produced by the martensitic transformation under shock, these two sets of dislocations interacting to form an extremely high dislocation density. When the shock pressure is removed, an entirely new set of dislocations must be produced in order for the high-pressure phase to revert to bcc. The shear process necessary for this reversion is prevented by the interaction of the existing dislocations. It is surprising that reversion of the high-pressure phase does not even occur when the specimens are cooled to liquid-nitrogen temperatures. Experiments will be performed to see if reversion occurs when specimens are cooled to 4.2 °K.

V. CONCLUSIONS

Based on the experimental findings of this work, shock deformation of quenched Fe-4Mn, Fe-7Mn, and Fe-14Mn results in a shock-induced phase transformation with the high-pressure phase retained upon relief. Furnace-cooled alloys up to 14 wt% Mn do not show retained close-packed phases after shocking. These results are explained by the conclusion that bcc iron with at least 4% Mn in solid solution will retain the close-packed phase produced by shock loading. The addition of manganese to iron also decreases the transition pressure from 133 kbar to less than 90 kbar for Fe-14Mn.

ACKNOWLEDGMENTS

This work was supported by the Defense Department through Advanced Research Project Association of the Department of Defense. A. Christou wishes to acknowledge the support of N.W.L. Independent Research funds. Shock loading was accomplished with the assistance of Dr. F.I. Grace and D. Altman. The authors also wish to acknowledge the assistance of Dr. S. Hooker for his helpful comments and assistance on the electron probe analysis, L. Flaer for his assistance in the density measurements, and D. Malyevac, head of the Materials Science Division, for his interest in the problem.

---

*Paper based on material submitted by Aristos Christou in partial fulfillment of the requirements for the degree of Doctor of Philosophy, University of Pennsylvania.

†Present address: Materials Science Division, U. S. Naval Weapons Laboratory, Dahlgren, Va. 22448.

[1]R. S. Davies, *Iron and Its Dilute Solid Solution* (Interscience, New York, 1963), p. 61.

[2]P. G. Johnson, B. A. Stein, and R. S. Davies, J. Appl. Phys. 33, 557 (1962).

[3]D. Bancroft, E. L. Peterson, and S. Minshall, J. Appl. Phys. 27, 291 (1956).

[4]R. N. Keeler and A. C. Mitchell, Solid State Commun. 7, 271 (1969).

[5]Troiano and S. F. McGuire, Trans. Am. Soc. Metals 31, 340 (1943).

[6]A. Christou, Phil. Mag. 21, 203 (1970).

[7]G. E. Duval and G. R. Fowles, *High Pressure Physics and Chemistry* (Academic, New York, 1963), p. 69.

[8]F. Rose, M. P. Villere, and T. L. Berger, Phil. Mag. 19, 39 (1969).

[9]R. Castaing, Advan. Electron. Phys. 13, 317 (1960).

[10]D. B. Wittry. University of Sourthern California Engineering Center Report No. 84-204, 1963 (unpublished).

[11]D.C. Brillhart, R.G. DeAngelis, A.G. Preban, J.B. Cohen, and P. Gordon, Trans. AIME, 239, 836 (1967).

[12]D.C. Brillhart, A.G. Preban, and P. Gordon, Trans. Am. Soc. Metals 1, 969 (1970).

[13]W.M. Lomer, Phil. Mag. 2, 1053 (1957).

[14]H. Kressel and N. Brown, J. Appl. Phys. 38, 1618 (1967).

[15]C. Sadron, Ann. Phys. (Paris) 17, 371 (1950).

[16]A. Christou, U.S. Naval Weapons Laboratory Technical Note No. TN-F-24/69, 1969 (unpublished).

[17]T. R. Loree, R. H. Warnes, E. G. Zukas, and C. M. Fowler, Science 153, 1277 (1966).

[18]H. G. Bowden and P. M. Kelly, Acta Met. 15, 1489 (1967).

[19]W. C. Leslie, D. W. Stevens, and M. Cohen, Second International Symposium on Materials, San Francisco, 1964 (unpublished).

[20]M. K. Koul and T. F. Breedis, *The Science, Technology, and Application of Titanium* (Pergamon, New York, 1969), p. 790.

[21]R. G. McQueen, E. Zukas, and S. Marsh, *Response of*

Metals to High Velocity Deformation (Interscience, New York, 1961), p. 106.
[22]L. Kaufman, A. Leyenaar, and J. S. Harvey, *Progress in Very High Pressure Research* (Wiley, New York, 1961), p. 90.